

Investigation of the photorefractive crystal based detection system for acousto-optic imaging (AOI) in highly diffuse media

Lei Sui^a, Ronald A. Roy^{*a}, Charles A. DiMarzio^{†b}, Florian Blonigen^b, and Todd W. Murray^{‡a}

Center for Subsurface Sensing and Imaging Systems

^aDepartment of Aerospace and Mechanical Engineering, Boston University,
110 Cummington Street, Boston, MA, 02215, USA

^bDepartment of Electrical and Computer Engineering, Northeastern University,
360 Huntington Avenue, Boston, MA, 02115, USA

ABSTRACT

Acousto-optic imaging (AOI) in diffuse media is a hybrid technique that is based on the interaction of multiply scattered laser light with a focused ultrasound beam. A phase-modulated optical field emanates from the interaction region and carries with it information about the local opto-mechanical properties of the insonated media. The goal of AOI is to reveal the optically relevant physiological information while maintaining ultrasonic resolution. Among the state-of-the-art optical detection techniques used for AOI, there is a trade-off between the axial resolution (or ultrasound bandwidth) and the signal-to-noise ratio (SNR). In this paper, a photorefractive-crystal (PRC) based interferometry system is employed to detect acousto-optic (AO) signals in highly diffuse media. This system allows for the use of short pulses of focused ultrasound and is capable of imaging mm-scale inhomogeneities imbedded inside tissue-mimicking phantoms. One-dimensional (1-D) sample imaging along the transducer axis is obtained from time-domain acousto-optic signal, where axial resolution is determined by the acoustic spatial pulse length, rather than the longer axial dimension of the ultrasonic focal region (as is the case when using a continuous-wave (CW) ultrasound source). Two-dimensional (2-D) images can be constructed through multiple 1-D line scans of the focused ultrasound transducer, which results in a reduction in imaging acquisition time and makes fast acousto-optic imaging possible.

Keywords: Acousto-optic imaging, photorefractive crystal, pulsed ultrasound, sensitivity, diffuse media

1. INTRODUCTION

Imaging biological tissues with light is very attractive not just because it is non-invasive and non-ionizing as opposed to X-rays, but also because it can provide valuable physiological and functional information, owing to the good optical contrast observed between normal and cancerous tissues.¹⁻² Difficulties in implementing pure optical imaging techniques³ arise from the fact that light propagation in soft tissues is typically dominated by multiple-scattering in the visible and near-infrared (NIR) wavelength range. This is especially true inside the so-called *therapeutic window* (650nm-1300nm), where the absorption coefficient of the overall tissue is minimal compared to the scattering coefficient. The highly diffuse nature of light propagation inside biological tissues blurs the optical images and compromises phase-coherent optical imaging techniques, resulting in a trade-off between imaging resolution and imaging depth.⁴ Consequently, it is difficult to achieve good optical imaging resolution (better than 1mm) inside biological samples at depth larger than 1cm. On the other hand, diagnostic ultrasound, one of the leading imaging modalities worldwide in clinical practice, achieves reasonably good imaging resolution at even greater imaging depths.⁵ However, diagnostic ultrasound has limited imaging ability to distinguish certain tissue types, e.g., non-palpable early-state tumors. This is due to the fact that the primary mechanism for ultrasound imaging contrast—bulk modulus, varies

* Prof. Ronald A. Roy, Email: ronroy@bu.edu; Phone: 617-353-4846;

† Prof. Charles A. DiMarzio, Email : dimarzio@ece.neu.edu; Phone : 617-373-8570;

‡ Prof. Todd W. Murray, Email: twmurray@bu.edu; Phone: 617-353-3951.

by only a few percent in soft tissues.⁶ In this context, several hybrid imaging techniques, showing promises in improving optical imaging resolution at larger imaging depth, have been proposed and are under investigation. These techniques include photoacoustic imaging (also called optoacoustic imaging),⁷⁻⁹ sonoluminescent tomography,¹⁰ and acousto-optic imaging (AOI),¹¹⁻²⁵ the latter of which is the subject of this paper. In AOI, a focused ultrasound beam is used to locally phase modulate or “tag” diffuse light through two main mechanisms: the periodic displacement of optical scattering sites and ultrasound-induced changes in refractive index.¹¹ The detection of this modulated light yields optically relevant physiological information with spatial resolution determined by ultrasound.

A great deal of work has been done since Dolfi and Micheron¹² patented the idea of photon frequency marking using ultrasound in 1989. Marks *et al.*¹³, in 1993, reported the tagging of diffuse laser light with pulsed focused ultrasound in a homogeneous scattering media. Leutz and Maret¹⁴ investigated the ultrasonic modulation of multiple light scattering speckles both experimentally and theoretically. Wang *et al.*¹⁵ and Kempe *et al.*¹⁶ demonstrated the utility of using the modulation of diffuse photons for imaging purposes. In order to enhance the signal-to-noise ratio (SNR), the former group employed a continuous-wave (CW) ultrasound source, and the modulated signals were detected using a single photomultiplier tube (PMT). Conventional single-detector techniques result in extremely low light levels when the detection aperture is limited to single speckle detection, and reduced modulation depth when the detection aperture is increased to receive multiple speckles (due to the random phase variations of the individual speckle grains of the output diffuse light field). To overcome the limitations of single detector techniques, Leveque *et al.*¹⁷ employed a multiple detector system based on a CCD array. The modulation amplitudes measured at each pixel element of the CCD are subsequently summed, leading to a substantial SNR increase over the single detector techniques. Utilizing this detection scheme, the authors demonstrated the detection of optically absorbing objects imbedded inside an ex vivo biological sample (turkey breast). Due to the slow response of the CCD camera, this parallel detection scheme is sensitive to any decorrelation of the speckle pattern that may occur during the measurement time. Recently, Gross *et al.*¹⁸ optimized the sensitivity of this parallel detection scheme using a heterodyne technique, and filtered out the speckle decorrelation noise with a spatial filter.

In most of the state-of-the-art AOI systems, a CW ultrasound source is employed, which allows for enhanced sensitivity through a reduction in detection bandwidth. However, the use of CW sources has its’ disadvantages. First of all, CW ultrasound based acousto-optic imaging affords very limited axial resolution. Also the use of CW ultrasound increases the potential deleterious bio-effects, such as excessive heating, that can result from the continuous high-intensity ultrasound exposure. Pulsed ultrasound permits significantly greater peak acoustic pressures while staying within Food and Drug Administration (FDA) exposure guidelines. Finally, narrow-band CW processing techniques are not compatible with conventional diagnostic ultrasound imaging machines which employ short-pulse ultrasound. To improve axial resolution for CW exposures, Wang and Ku¹⁹ introduced a frequency-swept method in which a single optical detector is used and the CW ultrasound source is chirped, thereby assigning a particular frequency to each location along the ultrasonic axis. A 1-D axial scan could then be produced from the frequency-domain information of the ultrasound-modulated signals. Because of the limited detection sensitivity of single-element detectors, this technique was initially demonstrated for ballistic imaging in clear and less diffuse media. Later, this chirp method was also combined with the CCD based parallel detection scheme to enhance axial resolution in highly diffuse media including biological tissues.²⁰⁻²¹ Alternatively, in the time domain, Lev and Sfez²² used pulsed ultrasound to “construct” CW signals by devising a reshaping algorithm to synchronize the ultrasonic pulses. Recently, the authors have designed a photorefractive-crystal (PRC) based interferometry system for the detection of ultrasound-modulated light in diffuse media. The method was shown to have sufficient sensitivity to detect the transiently modulated optical signals in the time domain, and thus supports the use of short-pulse ultrasound for acousto-optic imaging.²³⁻²⁵

In this paper, a single-sensor, PRC-based detection system is used to image optically absorbing targets imbedded inside highly diffusive tissue-mimicking phantoms. By using short pulses of focused ultrasound, one-dimensional images along the ultrasonic propagation axis are derived from the time-domain AO signal. To generate such a 1-D “line scan,” time is converted to distance by multiplying the elapsed time by the known speed of sound in the phantom. The axial and lateral resolution are determined by the ultrasound spatial pulse length and beam width, respectively. Two-dimensional acousto-optic images are also obtained by physically scanning of the transducer in a direction perpendicular to its axis. The succession of 1-D line scans, when displayed side by side, constitutes a 2-D planar image.

2. EXPERIMENTAL ARRANGEMENT

The experimental setup is shown in Fig. 1. A reference coordinate system is given, with the Z axis corresponding to the ultrasonic axis and the Y axis indicating the optical axis. A frequency doubled Nd:YAG laser source, with 80mW power and 532nm wavelength, is linearly polarized along Z axis and sent to a variable beam splitter where it is split into signal and reference beams with a power ratio of approximately 25:1. The reference beam is directed around the test tank and sent directly to the PRC. The signal beam is sent through a 10x beam expander to the water-submerged tissue-mimicking phantom via the flat glass wall of the tank. After passing through the sample, the scattered and ultrasonically modulated light is collected by a lens possessing an aperture of 5cm, and a focal length of 10cm. This collected light is directed into the PRC where it interferes with the reference beam at an angle of 20° . Our PRC detector employs a BSO crystal with dimensions of 5mm x 5mm x 7mm along the X, Z and Y axes, respectively, with a holographic cut along the [001], [110] and $[1\bar{1}0]$ directions. A 4-kHz, 10-kV/cm peak-to-peak AC field is applied to the crystal to enhance the grating strength and to improve the two-wave mixing gain ($\gamma \sim 0.2 \text{ cm}^{-1}$ under our experimental condition). After the PRC, the signal beam and diffracted reference beam (LO that is wave-front-matched to the signal beam) are sent through the other collection lens (aperture = 5cm, focal length = 10cm) and optical band-pass filter to an avalanche photodiode (APD) with a 10-mm diameter active aperture. The signal from the APD is amplified, low-pass filtered at 500 kHz, and sent to a digital storage oscilloscope that is triggered by the pulsed ultrasound signal generator. The time domain AO signal is coherently averaged (up to 10K sweeps) in order to achieve adequate SNR.

The sound source used to modulate the diffuse light is a single-element, spherically focused, piezoelectric transducer (Sonic Concepts, Bothell WA). It has a 6.3-cm focal distance and a 7.0-cm aperture. The central frequency of the transducer is 1.1 MHz and the bandwidth is 500 KHz. The ultrasonic axis is oriented vertically downward, perpendicular to the laser illumination direction. The transducer is mounted on a 3-D automated translation stage that is controlled by a personal computer via an RS-232 port. The transducer is driven using a pulse train possessing a center frequency of 1 MHz and a pulse repetition frequency (PRF) of 1 KHz. The pulse train is produced using a function generator, amplified by a fixed-gain power amplifier, and sent to an impedance matching box before the transducer.

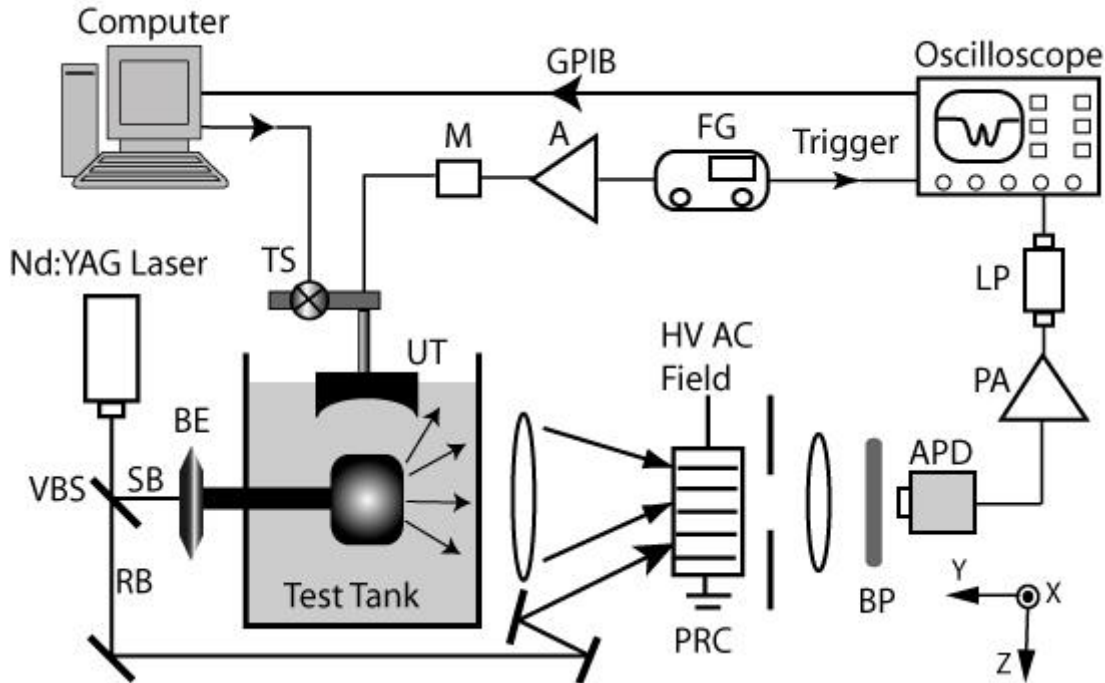


Figure 1. Experimental setup for PRC based detection of ultrasound modulated optical signals: FG- function generator, A- power amplifier, M- impedance matching box, TS- translation stage, UT- ultrasound transducer, VBS- variable beamsplitter, RB- reference beam, SB- signal beam, BE- beam expander, BP- optical bandpass filter, APD- avalanche photodiode, PA- preamplifier, LP- lowpass filter.

A tissue-mimicking gel phantom is submerged in a small glass tank filled with degassed and filtered water. The tank dimensions are $30\text{cm} \times 30\text{cm} \times 20\text{cm}$ along the X, Y and Z axes, respectively. The phantom consists of polyacrylamide gel fabricated using the recipe given in Ref. 23. Four hundred nanometer-diameter polystyrene microspheres are added to the gel during fabrication in order to modify the optical scattering coefficient; the particle-free gel is essentially transparent. The sound speed and the density of the phantom are measured to be about 1500 m/s and 1050 Kg/m^3 , matching approximately the acoustical properties of human breast tissue.²⁶ The dimensions of the phantom are $4\text{cm} \times 2.7\text{cm} \times 4\text{cm}$ (X, Y, Z). A $5\text{mm} \times 6\text{mm} \times 5\text{mm}$ (X, Y, Z) optical absorber is imbedded at the center of the phantom. The optical absorber consists of the same polyacrylamide gel with India ink is added to enhance the optical absorption coefficient; the ink has little effect on the acoustic properties of the material. Thus, we obtain a target imbedded in the gel possessing high optical absorption contrast and negligible acoustic contrast. A cut-away view of the phantom used in our experiment is shown in Fig. 2, with the reference coordinates indicated. The reduced scattering coefficient of the phantom is approximately 10 cm^{-1} .

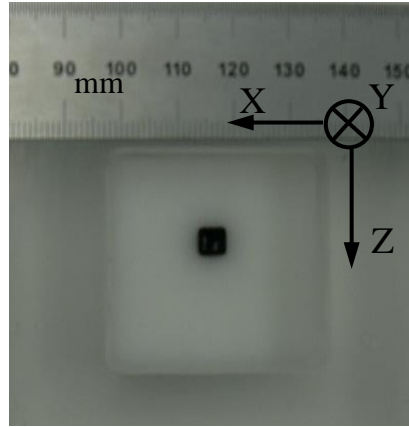


Figure 2. A photograph of a phantom slice ($4\text{cm} \times 4\text{cm}$) showing the imbedded optical absorber ($5\text{mm} \times 5\text{mm}$). The reduced scattering coefficient of the phantom is approximately 10 cm^{-1} . The optical absorber is fabricated using the exact same recipe as the surrounding phantom, except that India ink is added to adjust its absorption coefficient.

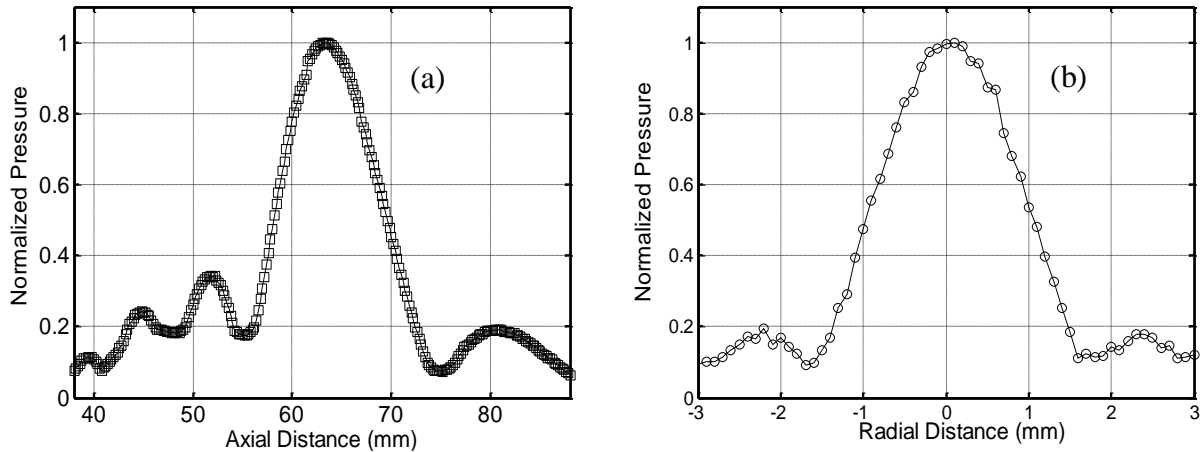


Figure 3. Experimental calibration of the transducer: (a) axial beam profile—normalized peak pressure vs. axial distance; (b) radial beam profile—normalized peak pressure amplitude vs. radial distance.

Lei, you need to add the radial axis of Figure 3, (b) so the labels are correct. 20 degrees

3. EXPERIMENTAL RESULTS AND DISCUSSION

The axial and radial (in the focal-plane) beam profiles of our transducer are shown in Fig. 3 (a) and Fig. 3 (b), respectively. The 3-D focal region, defined by the full-width-at-half-maximum intensity (FWHM), is a cigar-shaped ellipsoid with a long axis of about 9 mm and a short axis of about 1.5 mm. When driven CW, this focal region determines the axial and lateral imaging resolution. To improve the axial imaging resolution, we use *short pulsed ultrasound* instead of CW ultrasound. Fig. 4(a) shows a typical 2-cycle ultrasound pulse used in our experiment, corresponding to a spatial pulse length of ~ 3 mm and a peak negative pressure of ~ 0.63 MPa. These values fall well within the safe exposure limited imposed by the FDA for diagnostic ultrasound.^{5, 28} From Fig. 4 (a), one can clearly see the ring-down effect due to the finite bandwidth of the transducer. This spatial pulse length of ~ 3 mm is the minimum that our transducer can produce. Therefore, unless otherwise noted, a 2-cycle pulse was employed in all the experimental results shown below.

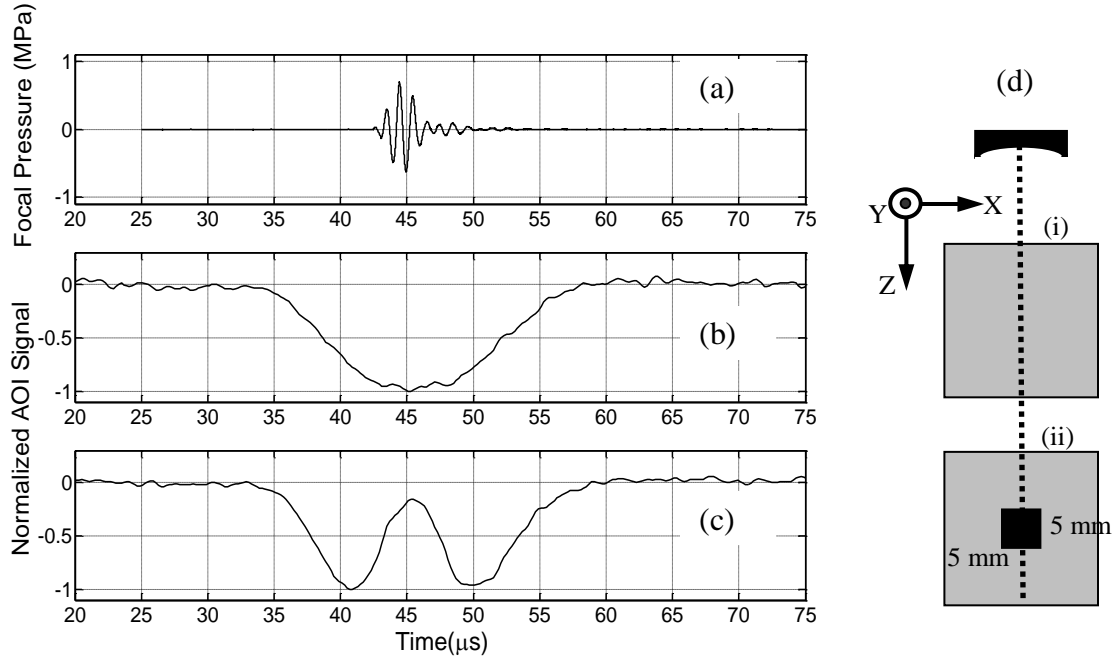


Figure 4. (a): The pressure output at the focus of the transducer measured by a needle hydrophone; (b) & (c): Typical acousto-optic (AO) signals detected for a homogeneous scattering phantom and a phantom with an optical absorber (5mm X 5mm) imbedded inside, respectively. These conditions correspond to schematic illustrations (i) and (ii) respectively.

In the experiments reported herein, the transducer is first scanned along X axis perpendicular to the optical source. Before scanning, the system is aligned to ensure that the center of the phantom roughly coincides with the center of the focal region of the transducer. The expanded signal beam is then directed at the middle of the front surface of the phantom. When the acoustic focal zone is the optical absorber (or a homogeneous scattering phantom is employed), the typical time-domain AO signal is shown in Fig. 4 (b). This signal is the so-called “DC offset” signal, which has been previously described in Refs 23-25. Fig. 4(c) shows a typical normalized DC offset signal obtained when the ultrasound beam traverses the optically absorbing target. These two scenarios are illustrated schematically in Fig. 4(d), where the incident laser beam (Y axis) is perpendicular to the page. When the ultrasound beam passes through the absorber, a peak is observed in the middle of the detected DC offset signal. The presence of the peak indicates that the strength of the AO interaction is diminished as the ultrasound pulse traverses the absorbing target; no phase modulated photons are detected because most of the light is absorbed. The signal observed when the ultrasound pulse beam does not traverse the absorber (Fig. 4(b)) does not show this feature.

The detected DC offset signal corresponds to the production of phase modulated photons generated as the ultrasound pulse travels down the acoustic axis. This time-domain record of the sample’s AO response can be converted to a space-domain “line scan” by multiplying the temporal coordinate by the speed of sound in the medium, as is typically

done in *B-mode* ultrasound imaging.⁵ A converted 1-D space-domain acousto-optic image is plotted in gray scale in Fig. 5(a), where the upper and the lower images correspond to the time-domain signals shown in Fig. 4(b) and Fig. 4(c), respectively. These images are 1-D “snapshots” of the acousto-optic interaction at points along the ultrasonic axis. This interaction is influenced by three factors: (1) the amplitude of the sound field, (2) the intensity of diffuse light, and (3) the optical characteristics of the medium. The acoustic pulse is essentially a probe traveling down the acoustic axis, broadcasting information related to the AO interaction over that region of space for which the optical field possesses sufficient intensity to yield a detectable DC offset signal. (For a tightly focused ultrasound source, this region will likely be further restricted to the focal zone of the transducer.) When launching a short-duration ultrasound pulse through a uniform medium, the DC offset signal essentially tracks the local light distribution along the ultrasonic axis, resulting in the broad peak shown in Fig. 4(b). Simply put, in order to get an AO signal from a given region, one must have *both* ultrasound and light coexisting in said region. If an optical absorber is present along ultrasound propagation path, it will absorb/trap any diffuse light passing through it locally, making it impossible for the modulated light to reach the detector and yielding the image contrast observed experimentally.

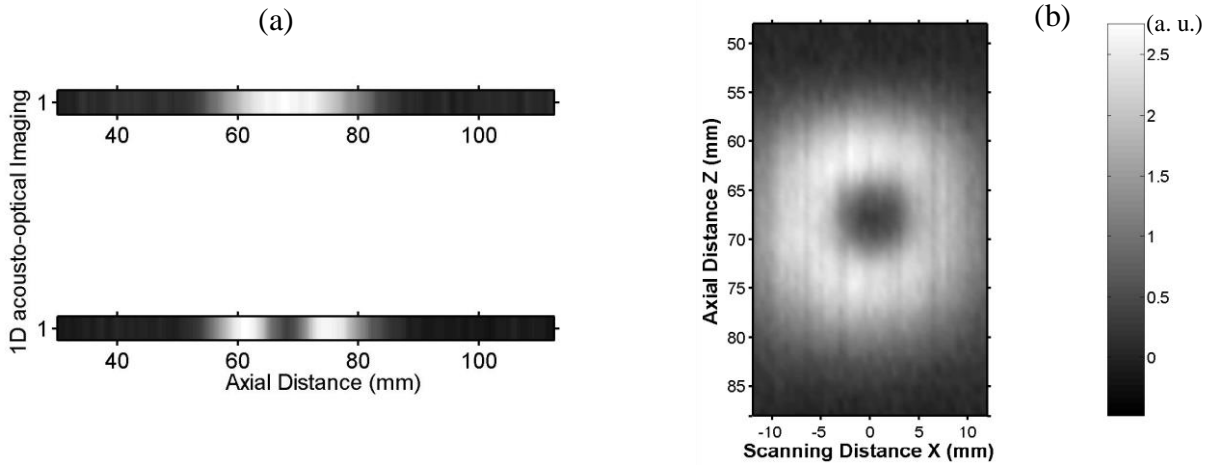


Figure 5. (a) 1-D acousto-optic images along the ultrasonic axis, where the upper and lower scans correspond to the cases of a homogeneous scattering phantom and an inhomogeneous one with 5mm absorbing target, respectively. (b) 2-D XZ-plane acousto-optic image of an optical absorber (5mm x 5mm) embedded inside a phantom with $\mu_s' = 10 \text{ cm}^{-1}$.

By scanning the acoustic transducer laterally along the X-axis, we generated a series of adjacent line-scan images which, when displayed simultaneously, resulted in the 2-D image (X-Z plane) shown in Fig. 5(b). In the middle section, a darkened region is readily seen, corresponding to the location of the optical absorber. The surrounding white area is the effective imaging area, corresponding to the illuminated region where the diffuse light interacts with the scanned ultrasound beam to generate a detectable signal. The tiny striations in the image are due to mechanical vibrations that are not completely compensated for by the PRC and lead to small variations in system sensitivity over the 2-D scan time.

Figure 5(b) demonstrates our ability to generate a 2-D image of an optical inhomogeneity by simply scanning the ultrasound beam along *one* axis, instead of two axes, a fact that affords a tremendous reduction in image acquisition time. For example, we currently average the transient AO signals up to 10K sweeps to get a SNR (defined by the maximum signal amplitude divided by the square root of the mean value of the noise amplitude squared) of $\sim 50:1$, which is proportional to $N^{1/2}$, where N is the number of coherent averaging. The current 1-D line-scan image along the ultrasonic axis at each scanning position takes about 10 seconds, and this time scales down with the number of averages and can be further reduced by increasing the acoustic PRF. Depending on the desired image quality, faster or even “real time” acousto-optic imaging is possible. For biomedical applications, this imaging technique could be potentially used for both “screening” (fast) and “imaging” (slow) purposes. Indeed, the use of short ultrasound pulses makes this technique adaptive to conventional diagnostic ultrasound imaging system, and makes a *direct* fusion of conventional diagnostic ultrasound and pulsed AOI possible.²⁹

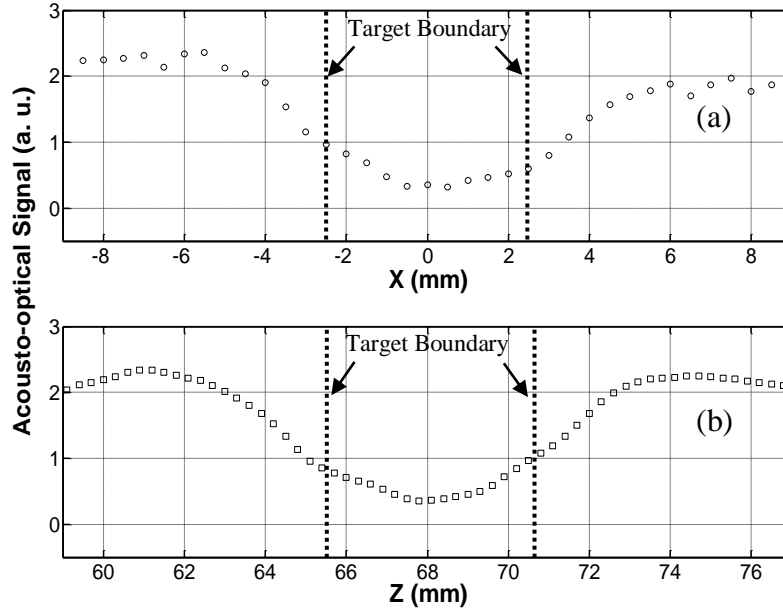


Figure 6. Close-up views of 1-D acousto-optic line-scan images across the center of the absorber in both X direction (a) and Z direction (b), corresponding to lines Z=68 mm and X=0 mm in Fig. 5 (b), respectively.

Figure 6 (a) and (b) show zoomed-in acousto-optic images across the center of the optical absorber in both X- and Z-directions. These plots clearly show that the AO images obtained in both directions are comparable to the actual target sizes (5mm x 5mm) as indicated by the [known] target boundaries. Secondly, if we define the imaging resolution by half the distance required for a decrease in optical contrast from 90% to 10% of the maximum, the optical imaging resolutions along X and Z directions are approximately 2mm and 2.5mm, respectively, which qualitatively matches the lateral dimension of the focal region (~1.5mm) and the spatial ultrasonic pulse length (~3mm). Finally, this also demonstrates that we can achieve spatial resolution in two dimensions. While the spatial pulse length primarily determines axial resolution, off-axis resolution is given by the width of the ultrasound beam. For focused sources, this is on the order of 2-3 wavelengths, thus, sub-millimeter pixel resolution is attainable if we employ higher ultrasound frequencies. Enhanced resolution is possible through the use of high frequency, broad-band ultrasound transducers commonly employed in commercial diagnostic imaging machines. Moreover, these machines employ electronic beam steering, further facilitating the generation of 2-D AO images. The fusion of AOI and diagnostic ultrasound was demonstrated previously.²⁹

4. CONCLUSIONS

The photorefractive-crystal-based interferometry system described above has sufficient sensitivity to detect pulsed-ultrasound modulated light for purposed of acousto-optic imaging in optically diffuse tissue phantoms. As described in Refs. 23-25, the PRC makes the detection of spatially incoherent phase modulation possible, where the resulting DC offset signal is dependent on the intensity of modulated light and the magnitude of the phase modulation. (The former is a function of optical absorption and the latter is a function of the acoustic pressure amplitude.) The adaptive nature of the PRC makes the system somewhat insensitive to speckle decorrelation on the time scale of the crystal response time. However, the response time of the crystal used in this study was 150 ms and some degree of vibration isolation was necessary. The use of a crystal with a faster response time could help to eliminate the speckle decorrelation problem altogether. By using short ultrasonic pulses, one-dimensional scan-line images of the targets positioned along the ultrasonic axis have been obtained through a single (averaged) time-domain acousto-optic waveform; the axial resolution is enhanced and determined by the spatial length of the ultrasound pulse. This fact makes high resolution attainable through the use of high frequency, broad-band ultrasound transducers. Two-dimensional imaging has also been demonstrated by mechanically scanning the transducer in one dimension, instead of two dimensions. This could

reduce the imaging acquisition time and make faster acousto-optic imaging possible. In addition, the use of short ultrasound pulses makes this technique adaptive to conventional diagnostic ultrasound, and makes a direct fusion of AOI with diagnostic ultrasound possible as will be shown in a companion paper published in this volume.³⁰

ACKNOWLEDGEMENT

The authors would like to acknowledge Dr. Emmanuel Bossy, Gopi Maguluri and Alex Nieva for valuable discussions. This work was supported by CenSSIS, *the Center for Subsurface Sensing and Imaging Systems*, under the Engineering Research Centers Program of the National Science Foundation (award number EEC-9986821).

REFERENCES

1. J. B. Fishkin, O. Coquoz, E. R. Anderson, M. Brenner, B. J. Tromberg., "Frequency-domain photon migration measurements of normal and malignant tissue optical properties in a human subject," *Appl. Opt.* **36**, 10-20 (1997).
2. B. Tromberg, N. Shah, R. Lanning, A. Cerussi, J. Espinoza, T. Pham, L. Svaasand, and J. Butler, "Noninvasive *in vivo* characterization of breast tumors using photon migration spectroscopy," *Neoplasia* **2**(1:2), 26-40 (2000).
3. V. V. Tuchin, ed., *Handbook of Optical Biomedical Diagnostics* (SPIE, Washington, 2002).
4. L. V. Wang, "Ultrasound-mediated biophotonic imaging: a review of acousto-optical tomography and photoacoustic tomography," *J. Disease Markers* **19** (3), 123-138 (2004).
5. T. L. Szabo, *Diagnostic Ultrasound Imaging: Inside Out* (Elsevier Academic Press, Boston, 2004).
6. S. Y. Emelianov, S. R. Aglyamov, J. Shah, S. Sethuraman, W. G. Scott, R. Schmitt, M. Motamedi, A. Karpouk, A. Oraevsky, "Combined ultrasound, optoacoustic and elasticity imaging," in *Photons Plus Ultrasound: Imaging and Sensing*, A. A. Oraevsky and L. V. Wang, eds. Proc. SPIE **5320**, 101-112 (2004).
7. A. A. Oraevsky and L. V. Wang, eds., *Proceedings of SPIE 5320—Photons Plus Ultrasound: Imaging and Sensing* (SPIE, Washington, 2004).
8. R. O. Esenaliev, A. A. Karabutov, and A. A. Oraevsky, "Sensitivity of laser opto-acoustic imaging in detection of small deeply embedded tumors," *IEEE J. Sel. Top. Quant.* **5**, 981-988 (1999).
9. X. Wang, Y. Pang, G. Ku, X. Xie, G. Stoica, and L. V. Wang, "Non-invasive laser-induced photoacoustic tomography for structural and functional imaging of the brain *in vivo*," *Nat. Biotech.* **21**, 803-806 (2003).
10. L. V. Wang and Q. Shen, "Sonoluminescence tomography of turbid media," *Opt. Lett.* **23**, 561-563 (1998).
11. L.-H. Wang, "Mechanisms of ultrasonic modulation of multiply scattered coherent light: an analytic model," *Phys. Rev. Lett.* **87**, 043903-(1-4) (2001).
12. D. Dolfi and F. Micheron, "Imaging process and system for transillumination with photon frequency marking," International Patent WO 89/00278 (1989).
13. F. A. Marks, H. W. Tomlinson, and G. W. Brooksby, "A comprehensive approach to breast cancer detection using light: photon localization by ultrasound modulation and tissue characterization by spectral discrimination," in *Photon Migration and Imaging in Random Media and Tissues*, B. Chance and R. R. Alfano, eds., Proc. SPIE **1888**, 500-510 (1993).
14. W. Leutz and G. Maret, "Ultrasonic modulation of multiply scattered light," *Physica B* **204**, 14-19 (1995).
15. L.-H. Wang, S. L. Jacques, and X.-M. Zhao, "Continuous-wave ultrasonic modulation of scattered laser light to image objects in turbid media," *Opt. Lett.* **20**, 629-631 (1995).
16. M. Kempe, M. Larionov, D. Zaslavsky, and A. Z. Genack, "Acousto-optic tomography with multiply scattered light," *J. Opt. Soc. Am. A* **14**, 1151-1158 (1997).
17. S. Leveque, A. C. Boccara, M. Lebec, and H. Saint-Jalmes, "Ultrasonic tagging of photon paths in scattering media: parallel speckle modulation processing," *Opt. Lett.* **24**, 181-183 (1999).
18. M. Gross, P. Goy and M. Al-Koussa, "Shot-noise detection of ultrasound-tagged photons in ultrasound-modulated optical imaging," *Opt. Lett.* **28**, 2482-2484 (2003).
19. L.-H. Wang and G. Ku, "Frequency-swept ultrasound-modulated optical tomography of scattering media," *Opt. Lett.* **23**, 975-977 (1998).
20. G. Yao, S. Jiao and L. V. Wang, "Frequency-swept ultrasound-modulated optical tomography in biological tissue by use of parallel detection," *Opt. Lett.* **25**, 734-736 (2000).

21. B. C. Forget, F. Ramaz, M. Atlan, J. Selb, and A. C. Boccara, "High-contrast fast Fourier transform acousto-optical tomography of phantom tissues with a frequency-chirp modulation of the ultrasound," *Appl. Opt.* **42**, 1379-1383 (2003).
22. A. Lev and B. G. Sfez, "Pulsed ultrasound-modulated light tomography," *Opt. Lett.* **28**, 1549-1551 (2003).
23. L. Sui, T. Murray, G. Maguluri, A. Nieva, F. Blonigen, C. DiMarzio and R. A. Roy, "Enhanced detection of acousto-photon scattering using a photorefractive crystal," in *Photons Plus Ultrasound: Imaging and Sensing*, A. A. Oraevsky and L. V. Wang, eds. Proc. SPIE **5320**, 164-171 (2004).
24. T. W. Murray, L. Sui, G. Maguluri, R. A. Roy, A. Nieva, F. Blonigen, and C. A. DiMarzio, "Detection of ultrasound-modulated photons in diffuse media using the photorefractive effect," *Opt. Lett.* **29**, 2509-2511 (2004).
25. L. Sui, R. A. Roy, C. A. DiMarzio, and T. W. Murray, "Imaging in diffuse media using pulsed-ultrasound-modulated light and the photorefractive effect," *Appl. Opt.* (accepted).
26. F. A. Duck, *Physical Properties of Tissue* (Academic, San Diego, 1990).
27. S. Leveque-Fort, "Three-dimensional acousto-optic imaging in biological tissues with parallel signal processing," *Appl. Opt.* **40**, 1029-1036 (2000).
28. R. E. Apfel and C. K. Holland, "Gauging the likelihood of cavitation from short-pulse, low-duty cycle diagnostic ultrasound," *Ultrasound Med. Biol.* **17**: 179-185 (1991).
29. E. Bossy, L. Sui, T. W. Murray, and R. A. Roy, "Fusion of conventional ultrasound imaging and acousto-optical sensing (AOS) using a standard pulsed ultrasound scanner," *Opt. Lett.* (in press).
30. E. Bossy, L. Sui, T. Murray, and R. Roy, "Combination of ultrasound and acousto-photon imaging using a pulsed ultrasound scanner," in *Photons Plus Ultrasound: Imaging and Sensing II*, A. A. Oraevsky and L. V. Wang, eds. Proc. SPIE **5697**-27 (to be published).